

FLEXURAL BEHAVIOR PREDICTION OF SFRC BEAMS: A NOVEL X-RAY TECHNIQUE

Sopokhem LIM^{*1}, Takehiro OKAMOTO^{*2}, Mitsuhiro MATSUDA^{*3}, and Mitsuyoshi AKIYAMA^{*4}

ABSTRACT

In the fabrication process, a number of parameters influence the distribution and orientation of fibers within individual structures. This phenomenon leads to a large scattering of flexural responses in SFRC beams. Consequently, prediction models of the flexural behavior of SFRC beams that do not consider the variability of fiber distribution often overestimate or underestimate the response. This paper presents a novel approach for estimating the flexural behavior of SFRC beams using X-ray photograms to account for the variability of the fibers.

Keywords: SFRC beam, X-ray technique, flexural behavior, spatial variability of fiber

1. INTRODUCTION

Steel fiber reinforced concrete (SFRC) is a material characterized by an enhanced post-cracking residual tensile strength due to crack-bridging stresses of fiber reinforcement. It is well known that the reliable and effective use of fibers in reinforcing concrete structures primarily depends on a uniform spatial distribution of fibers, oriented in the direction that counters the applied external stresses [1] and [2].

However, evidence from experimental research indicates that the fiber distribution is hardly uniform. In the fabrication process, a number of parameters influence the distribution and orientation of fibers within individual structures [3]. This phenomenon leads to highly scattered responses of post-cracking tensile strengths and prevents a reliable prediction of SFRC structural responses based on only fiber characteristics, fiber content, and the concrete matrix [4]. Consequently, prediction models regarding the flexural behavior of SFRC beams that assume the SFRC material as a homogenous material for simplification without consideration of the variation of fiber dispersion often overestimate or underestimate the flexural behaviors of SFRC members [5].

In this paper, the main objective is to establish a reliable method for predicting the flexural behavior of SFRC beams using X-ray images to account for the variability of the fibers' distribution and orientation in the individual members. In addition, the effect of a non-uniform fiber distribution on the flexural post-cracking residual strength is experimentally studied based on fiber distribution properties measured at a critical section. The validity of the prediction method is also presented. It is expected that this prediction method will provide a more reliable

estimation of the flexural performance of certain SFRC pre-cast members.

2. FLOWCHART OF THE ESTIMATION METHOD

Figure 1 shows a 6-step flowchart for estimating the flexural behavior of SFRC beams based on X-ray photograms. The first step is the measurement of the fiber number and distribution properties (i.e., orientation α_i , embedded length Le_i , and location Lo_i) in X-ray images captured at the critical plane of the notch location. The parameter known as the representative number of fibers, RNF, is defined by assigning the score of the roughly estimated pull-out strength performance to each fiber, considering its fiber properties. In the second step, the three-point beam bending test is performed to obtain the relationship between the load and the deflection (P- δ) and between the load and the crack mouth opening displacement (P-CMOD). In the third step, the two residual design strengths f_{R1} and f_{R3} corresponding to the loads F_1 and F_3 , respectively, are derived based on *fib* model code 2010. The relationship between the design strength parameters and RNF is established through a linear regression. From this relationship, f_{R1} and f_{R3} can be obtained using the distribution properties of the fibers measured in an X-ray image as an input. In the fifth step, a bilinear stress-crack width σ -w under uniaxial tension, which can be used to characterize the SFRC material, can be identified using f_{R1} and f_{R3} , and the tensile strength f_t can be estimated using the concrete compressive strength based on Wittmann [6]. Finally, the P- δ responses of the SFRC beams are predicted using the non-linear hinge model of Olesen [7]. In this model, the bilinear stress-crack width σ -w was used as the primary input parameter.

*1 Graduate School of Creative Sciences and Engineering, Waseda University, JCI Student Member

*2 Graduate School of Creative Sciences and Engineering, Waseda University

*3 Graduate School of Creative Sciences and Engineering, Waseda University

*4 Professor, Dept. of Civil and Environmental Engineering, Waseda University, JCI member

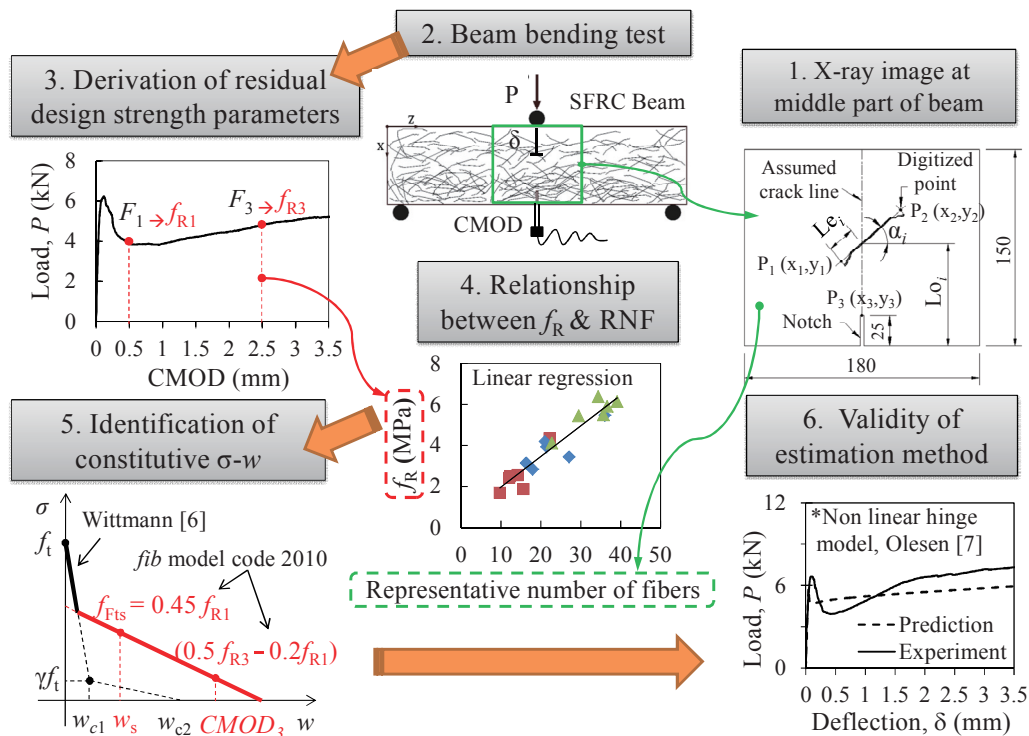


Figure 1. Flowchart for estimating the flexural behavior of SFRC beams based on X-ray images.

3. EXPERIMENTAL PROGRAM

3.1 Test specimens and materials

According to the above objective study, 3 series of specimens were fabricated. Each series comprised 6 beams (550 mm × 150 mm × 75 mm) and 3 cylinders (200 mm × 100 mm). The beam series F20, F30, and F40 contained fiber contents of 20 kg/m³, 30 kg/m³, and 40 kg/m³, respectively. The main characteristics of the fiber used are provided in Table 1. The mixing proportions of the concrete for the different beam series and the qualities of the materials are listed in Table 2.

Table 1 Characteristics of the fiber used herein.

Shape	L (mm)	Dia. (mm)	Young Modulus (GPa)	Tensile Strength (MPa)
	60	0.9	210	1225

Table 2 Mixing proportions of concrete per m³.

Water (kg)	Cement (kg)	F.A.* (kg)	C.A.† (kg)	Fiber (kg)	AE†† (ml)
189	420	619	1022	20	2940
189	420	619	1019	30	2940
189	420	619	1016	40	2940

*Fine aggregate with a specific density of 2.60 g/cm³ and a finess modulus of 2.64 g/cm³.

† Coarse aggregate ($G_{max} \leq 20$ mm) with a specific density of 2.64 g/cm³.

†† Air entrained agent.

3.2 Experimental procedure

(1) Specimen fabrication method

The concrete casting method according to [8] was used for the beam fabrication. Figure 3 shows the direction of concrete casting. The concrete was compacted by external vibration.

(2) X-ray radiography

X-ray radiography measurements were obtained using the configuration shown in Figure 2 to visualize and capture images of the fiber distribution within individual beams. The acquired X-ray photographs are 8-bit grey-scale images that consist of 1024 × 768 pixels. Figure 3 shows the area of the beam to be imaged by the X-ray apparatus as well as

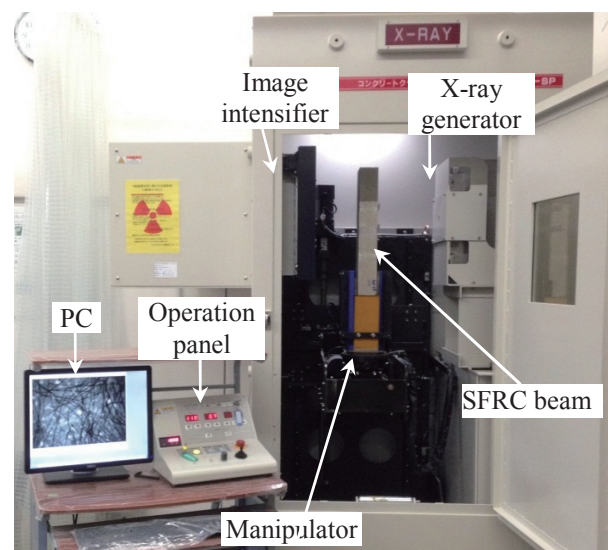


Figure 2. Configuration of the X-ray radiography measurement setup.

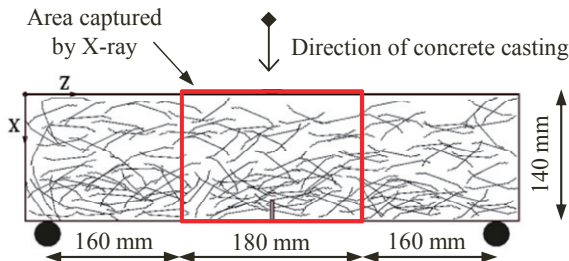


Figure 3. Area examined using the X-ray apparatus and direction of concrete casting.

(3) Beam bending test

On the 28th day, the mid-point bending test was performed, following the test setup shown in Figure 4. Two LVDTs were attached to the mounted steel plates on both sides of the beam to measure the two mid-span deflections of the beam. A clip gauge was also attached to the knife edges at the middle of the notch to record the crack mouth opening displacement (CMOD) or the crack width. Through trial-and-error tests, the beam bending test was conducted by maintaining the CMOD control at a rate of approximately 0.2 mm/min until completion of the test.

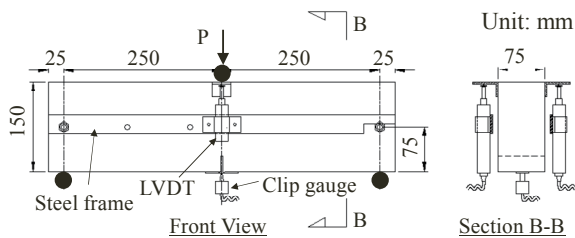


Figure 4. Three-point beam bending test.

4. EXPERIMENTAL RESULTS AND DISCUSSION

4.1 Effect of fiber content on the residual design strength parameters

Figure 5 shows the effect of fiber content on two post-cracking residual strengths, f_{R1} and f_{R3} , which were chosen as important design strength parameters characterizing a SFRC material, using the *fib* model code 2010.

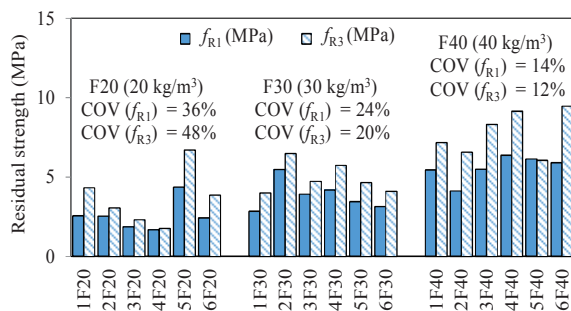


Figure 5. Effect of fiber content on residual strength.

Overall, a greater fiber content does not always lead to improved post-cracking residual strength. It can be observed that the residual strength of beam 5F20 is

higher than that of several beams in the F30 series and is even comparable to that of beam 2F40. Moreover, although the variability of residual strength decreases with increasing fiber content (i.e., average coefficient of variation (COV) values of 40%, 22%, and 13% for fiber contents of 20 kg/m³, 30 kg/m³, and 40 kg/m³, respectively), the strength variability within each series is significant. Therefore, it can be misleading to assess the flexural performance of SFRC members using only the fiber content.

4.2 Effects of non-uniform fiber distribution on the flexural behavior of the beam

Figure 6 shows the flexural responses of the F20 beam series, which is reinforced with a fiber content of 20 kg/m³. Despite utilizing the same batch of concrete and fabrication method, the beams in this series exhibit a large scatter of flexural post-cracking loads.

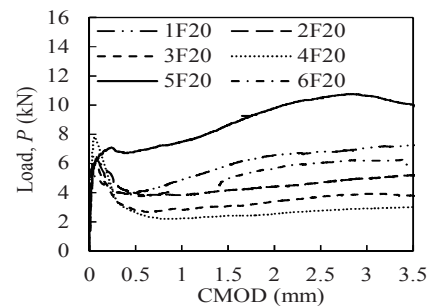


Figure 6. Relationship between the load and the CMOD for the F20 beam series.

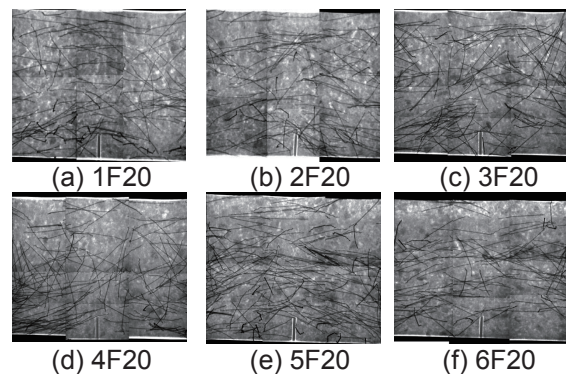


Figure 7. X-ray images of the F20 beam series.

This highly scattered response is due to the variability of fiber distribution and orientation inside the individual beams, as shown in the X-ray images in Figure 7. Figure 7(f) indicates that beam 5F20 had the highest number of fibers at the notch location. Thus, beam 5F20 exhibited a ductile behavior and withstood the highest post-cracking residual loads of the beams (see Figure 6). In contrast, Figures 7(d) and (e) indicate that beams 3F20 and 4F20 had the lowest number of fibers and thus exhibited brittle behavior and the lowest performance under post-cracking residual loads. These results demonstrate the fiber distribution at a critical section has a significant effect on the flexural post-cracking performance of SFRC beams.

5. ESTIMATION OF THE FLEXURAL BEHAVIOR USING X-RAY PHOTOGRAMS

5.1 Representative number of fibers

The experimental results reveal that the fiber distribution properties at the critical section significantly affect the flexural post-cracking strength during the pull-out process of fibers. The unknown fiber distribution properties and post-cracking residual strengths represent a challenge in reliably assessing the flexural performance of SFRC elements [4]. Therefore, it is necessary to create a parameter to account for the variability of fibers in each SFRC element, which can be obtained due to advances in X-ray technology that enable a visualization of the fiber distribution within the SFRC members. Firstly, the fiber distribution properties (i.e., orientation α_i , embedded length Le_i , and location Lo_i) of each fiber across the assumed crack line in X-ray photographs are measured via an advanced image analyzer (see Figure 8). The assumed score of a single fiber's pull-out performance as listed in Tables 3, 4, and 5 is assigned to each fiber depending on its measured values of α_i , Le_i , and Lo_i .

The representative number of fibers (RNF) for a beam can be determined by

$$RNF = \sum_{i=1}^k RNF_i = \sum_{i=1}^k \alpha_i \times Le_i \times Lo_i \quad (1)$$

where,

RNF_i : representative number of individual fiber across the assumed crack line

k : the number of fiber that locates across the assumed the crack line.

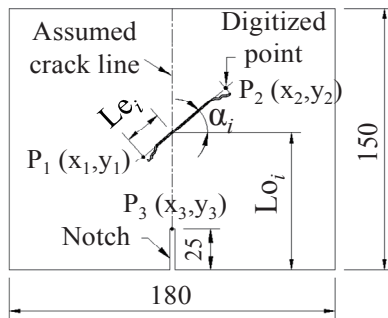


Figure 8. Measurement of fiber distribution properties.

5.2 Relationship between the fiber distribution properties and post-cracking design strength

The relationship between the flexural post-cracking residual strengths f_{R1} and f_{R3} and the RNF is established via linear regression analysis, as shown in Figures 9 (a) and (b), respectively. The relation coefficients of $R^2 = 0.89$ and $R^2 = 0.70$ demonstrate a strong relationship between the post-cracking design parameters and the RNF. This relationship enables the derivation of post-cracking residual strengths f_{R1} and f_{R3} using only the measured fiber distribution properties, based on RNF, with the X-ray image as the input.

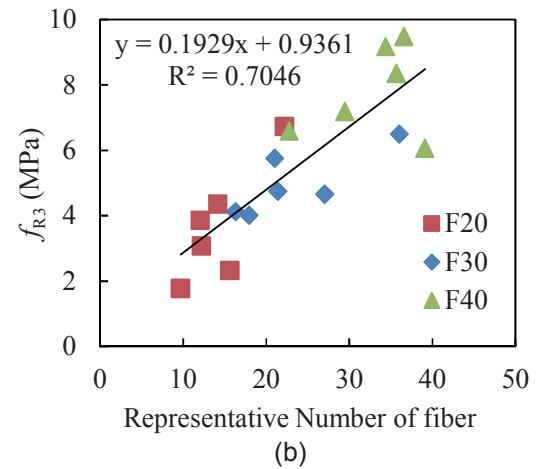
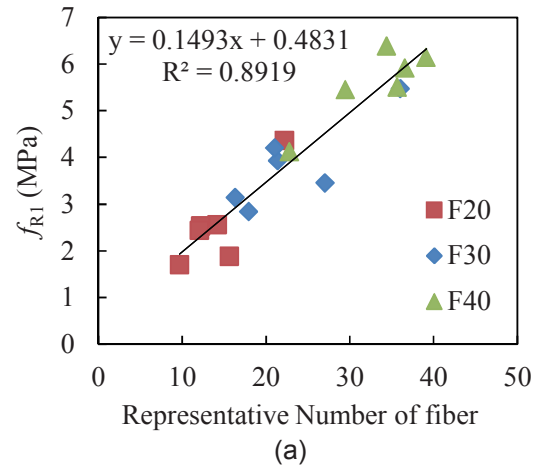


Figure 9. Relationship between the RNF and the post-cracking residual strengths.

Table 3. Assumed score for the fiber angle.

Angle (α_i)	0°~10°	10°~20°	20°~30°	30°~40°	40°~50°	50°~60°	60°~70°	70°~80°	80°~90°
Score	95%	92.50%	90%	80%	70%	65%	30%	15%	5%

Table 4. Assumed score for the fiber location.

Location (Lo_i)	25~50 mm	50~75 mm	75~100 mm	100~125 mm	125~150 mm
Score	100%	100%	100%	50%	50%

Table 5. Assumed score for the embedded length of the fibers.

Embedded length (Le_i)	≤ 50 mm	≥ 10 mm
Score	25%	100%

5.3 Identification of the constitutive stress-crack opening relationship

A bilinear stress-crack width σ - w , as shown in Figure 10, is used to characterize the SFRC material under uniaxial tension. This constitutive relationship can be identified using the residual design strength parameters f_{R1} and f_{R3} , which can be obtained from the above-described regression relationship using RNF as the input, and the tensile strength f_t , which can be estimated using the concrete compressive strength based on Wittmann [6]. The bilinear model is a combination of (1) a slope representing the constitutive σ - w relation for the concrete, as derived following Wittmann [6], and (2) a second slope representing the linear post-cracking constitutive σ - w relation for steel fiber, in accordance with the *fib* model code 2010. This bilinear constitutive model provides the main input parameters for the non-linear hinge model of Olesen [7]

5.4 Validity of the prediction method

The validity of the prediction method is verified by comparing the predicted P - δ responses with those obtained from the experiment as shown in Figure 11.

It can be seen that the predicted results are in good agreement with the experimental findings for beams 1F20, 4F30, and 4F50, as shown in Figures 11 (a), (c), and (d), respectively, independent of the fiber content. However, there are also a few discrepancies, particularly overestimated responses, as in the case of beam 2F20 in Figure 11(b). This result indicates that the estimation method requires further improvement.

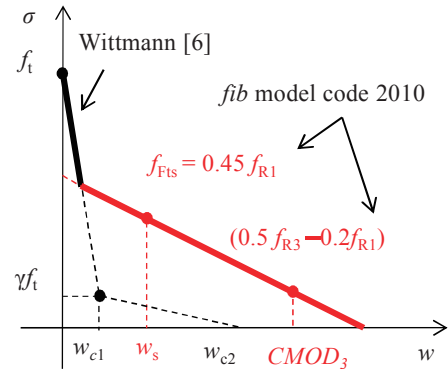
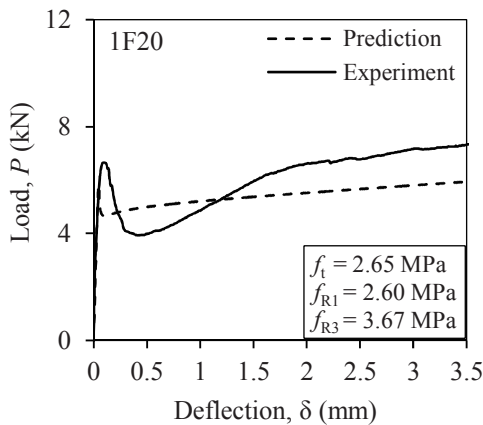
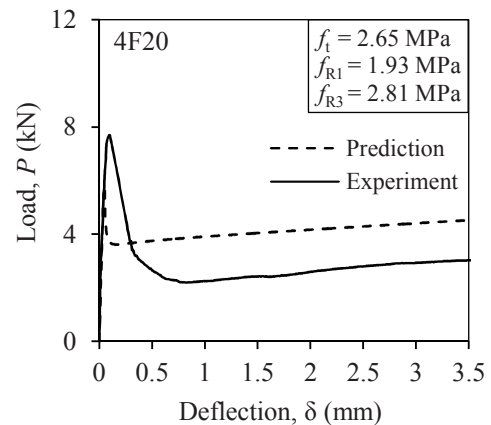


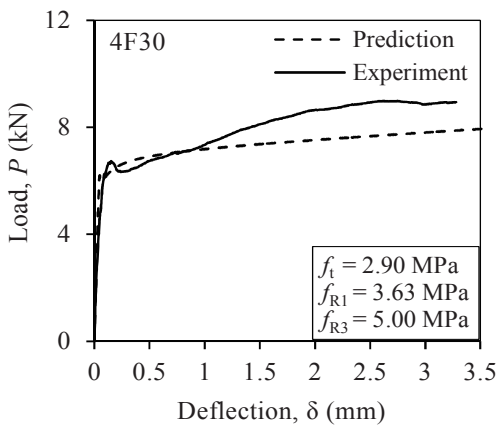
Figure 10. Constitutive stress-crack opening relationship of SFRC material.



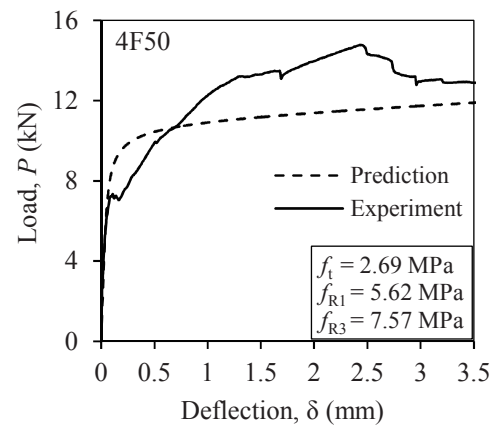
(a) 1F20



(b) 4F20



(c) 4F30



(d) 4F50

Figure 11. Comparison of predicted and experimental P - δ responses.

6. CONCLUSIONS

A procedure for predicting the flexural behavior of SFRC beams using X-ray photograms was presented, and its validity was confirmed. The following conclusions can be drawn from this study:

- (1) Based on the experimental results of three series of 6 SFRC beams that follows the same fabrication method, the variability of the post-cracking strength decreases with increasing fiber content. However, an increased fiber content does not always result in improved flexural residual strength.
- (2) The large scatter of the flexural post-cracking responses of SFRC beams was found to be significantly affected by the non-uniform distribution or variability of fibers within individual members.
- (3) In the prediction method, the variability of fiber dispersion in each beam was considered using the representative number of fibers, which is obtained from the fiber distribution properties measured in X-ray images. Although some predicted results were found to compare well to those obtained experimentally, overestimations occurred in a few cases. This result indicates that the prediction method requires further improvement.

In this research, the angle effect of fiber in the direction of the beam width was not considered since its effect might not be significant due to the ratio of fiber length to the beam width ($= 0.75$). However, it should be noted this is one of drawbacks for the present method which requires more improvement for the future researches, especially when the beam with larger width will be analyzed.

ACKNOWLEDGEMENT

The authors express sincere appreciation to Mr. Gan Cheng Chian at BEKAERT Singapore Pte Ltd. and Dr. Hexiang Dong at BEKAERT Japan Co., Ltd. for their kind supports and cooperation for this experiment. The options and conclusions presented in this paper are those of the authors and do not reflect the views of the sponsoring organizations.

REFERENCES

- [1] Ferrara, L., Park, Y.D., and Shah, S.P. "Correlation among fresh state behavior, fiber dispersion, and toughness properties of SFRC" *Journal of Material Civil Engineering*, Vol. 20, pp. 493-501.
- [2] Stahli, P., Custer, R., and Mier, J.G.M.V. "On Flow Properties, Fibre Distribution, Fibre Orientation and Flexural Behaviour of FRC" *Materials and Structures*, 2008, Vol. 41, pp. 189-196.
- [3] Edgington, J., and Hannant, D. J. "Steel fiber reinforced concrete. The effect on fiber orientation of compaction by vibration," *Materials and Structures*, Vol. 5, 1972, pp. 41-44.
- [4] di Prisco, M., Colombo, M., and Dozio, D. "Fibre-reinforced concrete in *fib* Model code 2010: principles, models and test validation." *Structural Concrete*, 2013, Vol.14, pp. 342-361.
- [5] de Montaignac, R., Massicotte, B., and Charron, J-P. "Design of SFRC Structural Elements: Flexural Behavior Prediction." *Materials and Structures*, 2012, Vol. 45, pp. 623-636.
- [6] Wittmann, F.H. , Roelfstra, P.E., Mihashi, H., Huang, Y-Y., Zhang, X-H., Nomura, N. "Influence of age, water-cement ratio and rate of loading on fracture energy of concrete". *Materials and Structures*, 1987, Vol.20, pp. 103-110.
- [7] Olesen, JF. "Fictitious Crack Propagation in Fiber-Reinforced Concrete Beams." *Journal of Engineering Mechanics*, ASCE, 2001, Vol.127, pp. 272-280.
- [8] RILEM TC 162-TDF "Test and design method for steel fiber reinforced concrete. Bending test, final recommendation". *Materials and Structures*, 2002, Vol.35, pp. 579-582.